Solvent mobility and the protein 'glass' transition

Dennis Vitkup[1–3], Dagmar Ringe[1,4], Gregory A. Petsko[1,4] and Martin Karplus[3,5]

[1]Rosenstiel Basic Medical Sciences Research Center, Brandeis University, Waltham, Massachusetts 02454-9110, USA. [2]Department of Biology, Program in Biophysics and Structural Biology, Brandeis University, Waltham, Massachusetts 02454-9110, USA. [3]Department of Chemistry and Chemical Biology, Harvard University, Cambridge, Massachusetts 02138, USA. [4]Department of Chemistry and Department of Biochemistry, Brandeis University, Waltham, Massachusetts 02454-9110, USA. [5]Laboratoire de Chimie Biophysique, Institut le Bel, Universite Louis Pasteur, 67000 Strasbourg, France.

Proteins and other biomolecules undergo a dynamic transition near 200 K to a glass-like solid state with small atomic fluctuations. This dynamic transition can inhibit biological function. To provide a deeper understanding of the relative importance of solvent mobility and the intrinsic protein energy surface in the transition, a novel molecular dynamics simulation procedure with the protein and solvent at different temperatures has been used. Solvent mobility is shown to be the dominant factor in determining the atomic fluctuations above 180 K, although intrinsic protein effects become important at lower temperatures. The simulations thus complement experimental studies by demonstrating the essential role of solvent in controlling functionally important protein fluctuations.

The internal motions of proteins are essential for their function[1,2]. Thus, an understanding of protein dynamics is of fundamental importance to biology. Protein dynamics is determined by the protein energy surface — a function describing how the energy of the protein varies as the structure changes. For protein configurations similar in structure to the native state, the energy surface is known to have multiple minima (substates) and the protein motions at ambient temperatures have been shown to involve both harmonic displacements within the minima and crossing of the barriers between them[3,4]. These conformational substates have different functional properties[5].

Experiments and theory suggest that the protein energy surface is similar to that of disordered media, such as glasses[5,6]. Like glass-forming liquids[6,7], proteins in the native state have been shown to undergo a dynamic transition (usually referred to as the 'protein glass transition') at ~200 K (refs 8–12). The transition is manifested by a reduction in the magnitude and an increase in the time scale of the atomic fluctuations[11–13]. The dynamic transition has been demonstrated by a variety of experimental techniques, including rebinding studies of small ligands in myoglobin[14], X-ray crystallography[10], neutron scattering[11], and Mössbauer scattering[15,16]. Recently, a dynamic transition, similar to that of proteins, was found in DNA[17]. Myoglobin[14], ribonuclease[10], elastase[18], and bacteriorhodopsin[19] were shown to be inactive below the transition temperature. Molecular dynamics simulations of proteins and DNA at a series of temperatures in vacuum and in the presence of explicit solvent[12,13,20] have shown relatively abrupt changes in the amplitude and time scale of the atomic fluctuations that are in accord with experimental studies of the 'glass' transition in biomolecules.

Because the 'glass' transition appears to be an essential feature of protein dynamics and affects the function of proteins with diverse biochemical roles and mechanisms, it is important to understand its origin. The energy surface of a protein, like that of any solute, is determined by the internal potential energy surface (the energy surface that would be calculated for a protein *in vacuum*, with no surrounding solvent) and the perturbations due to the solvent[21]. The solvent could alter the free energy of the protein to create an effective potential energy surface, or it could have more direct dynamic effects as a result of collisions between solvent molecules and the protein atoms[21,22]. Thus, the temperature dependence of the motions on both the effective protein energy surface and the solvent mobility could contribute to the transition.

The original observation of nonexponential geminate rebinding kinetics of carbon monoxide (CO) to myoglobin at temperatures below 160 K was interpreted to result from an inhomogeneous population of protein molecules that were frozen in different conformational substates[5,14] (in kinetic studies, geminate rebinding refers to rebinding of the same ligand molecule from within the protein). The assumption was that below the transition, the rates of interconversion among the conformational substates are slow relative to CO rebinding primarily due to the barriers separating these states on the effective energy surface. An alternative possibility is that the protein 'glass' transition, as manifested in non-exponential rebinding, is a consequence of the solvent glass transition. In this scenario, the solvent motions become so slow that individual protein molecules are trapped in different solvent cage configurations and cannot undergo the conformational relaxation necessary for CO rebinding. The latter view is consistent with the fact that the rate of protein conformational relaxation, as measured by changes in the heme absorption spectrum after CO photodissociation, can be slowed by highly viscous solvents even at room temperature[23–25]. From these results, it was concluded that protein motion below the dynamic 'glass' transition is inhibited predominantly by high solvent viscosity rather than by an inability of the protein to cross over the potential energy barriers due to the lack of kinetic energy. Experiments on hydrated carboxymyoglobin films showed that conformational transitions between different states of bound CO could be observed down to 80 K (ref. 26). Thus, the absence of solvent capable of undergoing the 'glass' transition in these experiments seems to explain why the conformational transitions were observed. This conclusion is consistent with the measurements of bound CO state transition rates as a function of temperature, which indicate that the dynamic behavior of the protein is correlated with a glass transition in the surrounding solvent[8]. However, neutron scattering measurements of hydrated myoglobin powder samples (powder samples that have been allowed to absorb some moisture but not enough to redissolve the protein) indicate a transition in both the magnitude and time scale of atomic fluctuations in the protein. These results were interpreted as being related to the role of torsional transitions in protein fluctuations (that is, the effective potential surface[27]). In addition, the dynamic 'glass' transition observed in molecular dynamic simulations in vacuum[12], as well as in simulations with explicit solvent[13,20], suggests that the internal potential energy surface can play a role.

Here we use molecular dynamics simulations to study the 'glass' transition and separate the effects of the protein potential surface and of solvent mobility on the atomic fluctuations. The approach makes use of the fact that different parts of a simulation system can be kept at different temperatures and that the amplitudes of the protein fluctuations can be monitored as a function of the protein and solvent temperatures. Specifically, the Nose-Hoover thermostats[28] make it possible to constrain the two parts of the simulation system to different effective temperatures (defined by the average velocity of the atoms). Four different systems were initially investigated — protein atoms at 180 K and solvent atoms at 180 K (PC/SC), protein atoms at 180 K and solvent atoms at 300 K

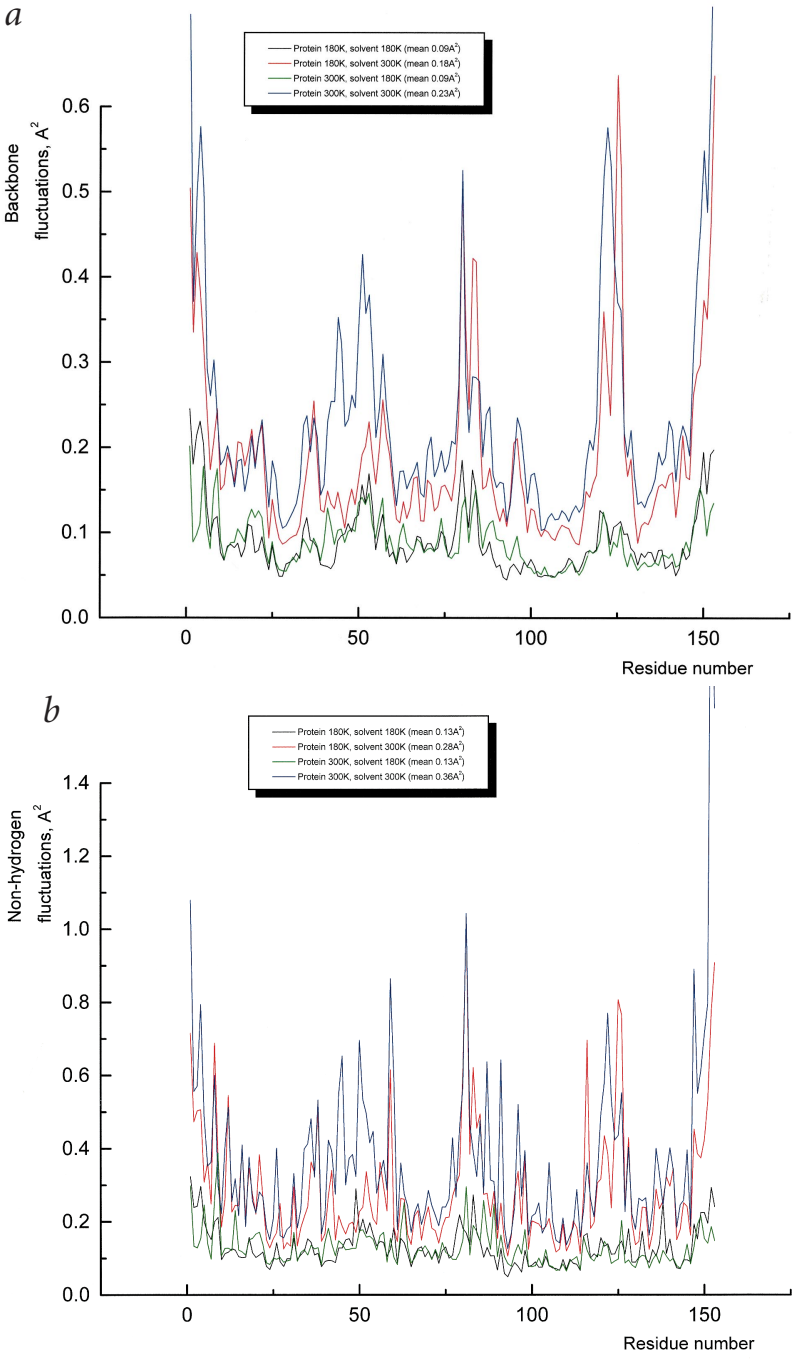

Fig. 1 Atomic fluctuations *versus* residue number. Atomic fluctuations from Nose-Hoover simulations of myoglobin and the water solvation shell system (see Methods for description of Nose-Hoover simulations); mean square atomic fluctuations were averaged over the atoms within each residue. Protein at 180 K and solvent at 180 K (black); protein at 180 K and solvent at 300 K (red); protein at 300 K and solvent at 180 K (green); protein at 300 K and solvent at 300 K (blue). ***a***, Profile of average residue backbone fluctuation *versus* myoglobin residue number. ***b***, Profile of average residue non-hydrogen fluctuation *versus* myoglobin residue number. Note that the fluctuation profiles are similar in pairs for which water is coupled to the same temperature, independent of protein temperature. Figs. 1–3 were generated using MicroCal Origin 5.0 (Microcal Software, Inc.).

(PC/SH), protein atoms at 300 K and solvent atoms at 180 K (PH/SC), protein atoms at 300 K and solvent atoms at 300 K (PH/SH); the symbols P and S stand for protein and solvent, and H and C for hot and cold. There are two standard simulations: below (PC/SC) and above (PH/SH) the protein 'glass' transition. The (PH/SC) simulation mimics the experimental study of Hagen *et al.*[25] in which the room temperature protein is in a high viscosity solvent. Finally, the (PC/SH) simulation is a crucial one that is not directly related to any experiment but permits one to determine the behavior of a protein whose temperature is below the glass transition in the presence of a low viscosity (high temperature) solvent.

The backbone and all non-hydrogen atom fluctuations as a function of residue number from the four different systems are shown in Fig. 1*a*,*b*, respectively. The corresponding average backbone and all non-hydrogen atom mean square fluctuations are given in Table 1 for comparison. The results are striking: the atomic fluctuations are almost identical for simulations in which water molecules are at the same temperature, independent of the temperature of the protein; that is, the PH/SH and PC/SH simulations are very similar, as are the PH/SC and PC/SC simulations. In the PC/SH simulation, the protein atoms have a kinetic energy corresponding to a temperature below the reported 'glass' transition but, due to the solvent mobility, the protein fluctuations are almost identical to those at 300 K. On the other hand, if the solvent temperature is below the glass transition, the protein fluctuations are significantly reduced, independent of the protein temperature and kinetic energy. These results suggest that for myoglobin, the 'glass' transition is governed chiefly by the solvent in this temperature range.

Elber and Karplus[3] demonstrated that the motions of myoglobin that make the dominant contributions to atomic fluctuations involve transitions between minima (substates) corresponding to nearly rigid helix reorientations coupled with interhelical side chain and loop rearrangements. The average mutual distance and angle fluctuations of adjacent myoglobin helices in four Nose-Hoover trajectories are given in Table 1. The fluctuations in secondary structure angles and distances are strongly coupled to solvent mobility; that is, they are large for the SH and SC simulations, independent of the protein temperature. This is in accord with the fact that the fluctuations as a function of residue number are much more uniform in SC simulations than in SH simulations; that is, the profile with characteristic maxima found in the free water simulations (Fig. 1) and from experimental Debye-Waller factors (B-factors) is essentially absent. (The Debye-Waller factor is the number that can be assigned to every atom in a protein crystal structure by fitting a Gaussian function to the spreading of electron density that is observed around the equilibrium position of that atom. Although both static and dynamic disorder contribute to this spreading of electron density, for many proteins dynamic effects are very important and therefore, the B-factors are a reflection of the mobility of the atom.) Maxima in the experimental Debye-Waller factors and simulation profile often correspond to mobile surface residues (for example, those in loops), whose motions are restricted by the glass-like solvent[29].

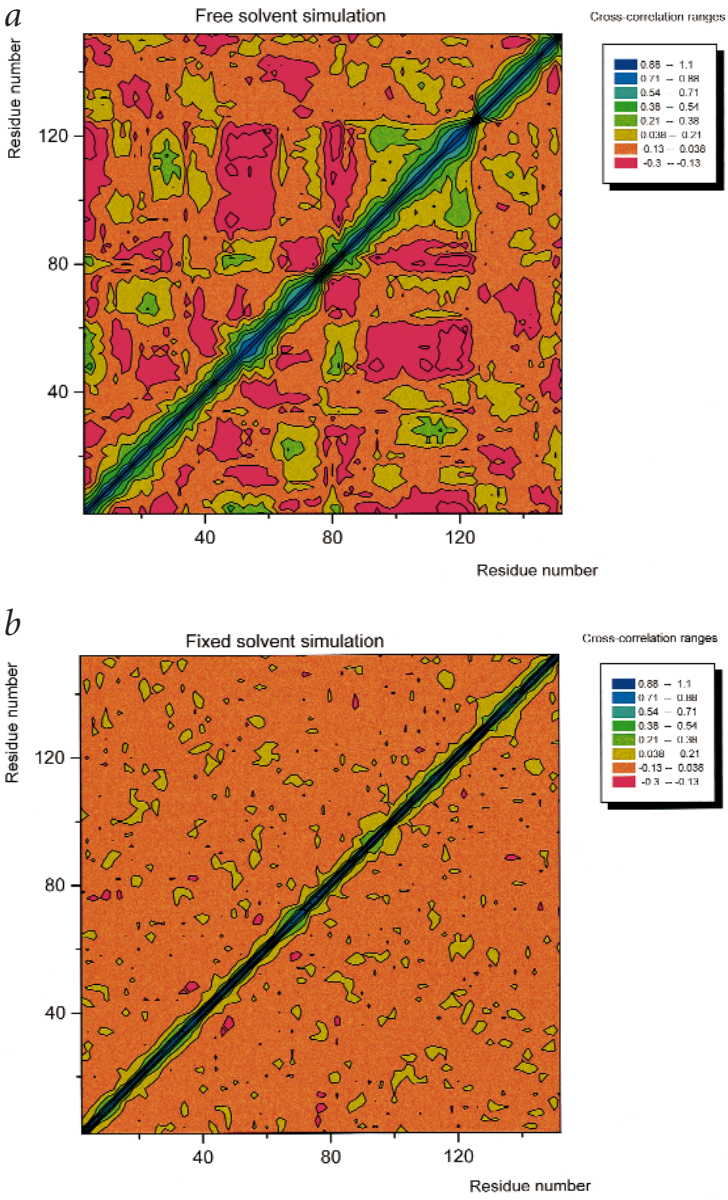

Fig. 2 Cross correlation of atomic fluctuations, averaged by residue over backbone protein atoms. Cross correlation ranges are indicated by different colors. The same simulation system and protocol as in Nose-Hoover simulations were used; simulations were done at 300 K. Before cross correlation analysis, trajectory frames were superimposed with MBCO crystal structure[37] to remove overall translation and rotation motion. Cross correlation between atoms i and j for molecular dynamic trajectory is calculated using the formula:

$$C(i,j) = (\langle \Delta R(i) \times \Delta R(j) \rangle) / (\langle (\Delta R(i))^2 \rangle^{1/2} \times \langle (\Delta R(j))^2 \rangle^{1/2})$$

where $\Delta R(i)$ and $\Delta R(j)$ are displacements for atoms i and j and averaging is done over the trajectory frames[32]. ***a***, Backbone cross correlation for free water trajectory. ***b***, Backbone cross correlation for fixed water trajectory

The backbone and side chain bond length and bond angle fluctuations, by contrast, are determined mainly by the intrinsic protein temperature; that is, the bond length and bond angle fluctuations are similar in the PH/SH, PH/SC, and PC/SH, PC/SC pairs (Table 1). This result demonstrates that while global fluctuations are governed by solvent mobility down to at least 180 K, local fluctuations are mostly determined by the intrinsic protein potential and the atomic kinetic energy. The fast convergence of the fluctuation magnitudes in the low temperature solvent indicates that the motions are restricted to a single minimum and that the global distortions, which involve transitions between minima, are absent. This is in accord with studies by Swaminathan *et al.* on BPTI[30], which showed that the fast fluctuations are uniform throughout the protein and that longer time motions introduce the characteristic inhomogeneity.

To determine the nature of the interactions between water and the protein responsible for freezing the protein motions at ~200 K, myoglobin simulations in a box of water molecules with charges set to zero were performed (data not shown). The simulations showed that electrostatic and hydrogen bonding interactions between water molecules and the protein are mainly responsible for the 'freezing out' of collective protein fluctuations at low temperature. The interpretations of inelastic neutron scattering studies of hydrated and dehydrated myoglobin also stressed the importance of hydrogen bonding interactions[31].

As a limiting case of a glass-like solvent, molecular dynamics simulations at room temperature were performed with fixed water molecules in the first hydration shell. Three simulations were performed with the water positions taken from well separated frames of a 300 ps molecular dynamics simulation of CO bound myoglobin at 300 K (D.V., D.R., G.A.P. and M.K., unpublished results). The protein fluctuations were found to converge in less than 10 ps, compared with 50 ps for solvent at 180 K and more than 100 ps for solvent at 300 K. The same results were obtained from the three simulations, indicating that they are independent of the fixed solvent positions around the protein and that the important element is that the solvent is fixed, as it would be in a rigid glass. The mean square atomic fluctuations of the protein in fixed solvent are about four times smaller than those in the room temperature solvent for the backbone and all non-hydrogen atoms (Table 1). The local motions (bond length and bond angle fluctuations), which can occur without distortions of the protein surface, are still present and are similar to the PH/SH and PH/SC values.

Another functionally important characteristic of protein motions is the cross correlation between the atomic fluctuations[32]. Cross correlation analysis demonstrates if atomic motions are correlated (positive correlation), anticorrelated (negative correlation), or uncorrelated (zero correlation). Comparison of the fixed water and free water simulations at 300 K (Fig. 2*a*,*b*) shows that the rich pattern of correlated and anticorrelated motion present in the former (Fig. 2*a*) is basically absent in the latter (Fig. 2*b*). In fixed water simulations all inter-residue 'communication' is lost. Based on the principle component analysis (which determines the directions of the protein motions with the largest amplitudes), the fixed solvent protein dynamics was found to be globally harmonic even at ambient temperature. Motions along largest principle components observed in free solvent simulations are dampened in the fixed solvent.

Fluctuations of non-hydrogen protein atoms as a function of distance to the protein surface are shown in Fig. 3. Because protein surface atoms are essentially completely frozen in the fixed water simulations, the protein fluctuations decrease from the

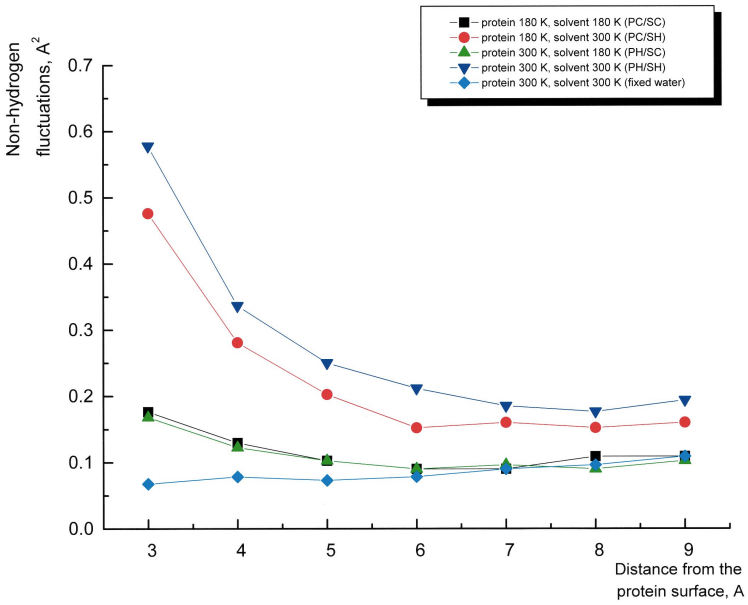

Fig. 3 Mean square fluctuations as a function of distance from the protein surface. Mean square fluctuations of non-hydrogen myoglobin atoms as a function of distance from the protein surface for the Nose-Hoover and fixed water simulation. Protein at 180 K, solvent at 180 K (black); protein at 180 K, solvent at 300 K (red); protein at 300 K, solvent at 180 K (green); protein at 300 K, solvent at 300 K (blue); fixed water, protein at 300 K (cyan). Myoglobin non-hydrogen atoms were grouped together based on the distance from the protein surface in the crystal structure[37]; the distance groups used are: atoms located within 3.5 Å of the surface, 3.5–4.5 Å, 4.5–5.5 Å, 5.5–6.5 Å, 6.5–7.5 Å, 7.5–8.5 Å, and 8.5–9.5 Å from the surface. Atomic fluctuations were averaged for atoms within each group. Non-hydrogen atom fluctuations in the protein core are similar for the fixed water trajectory and the trajectories in which water was kept at 180 K.

core to the surface. In all other simulations, as in experiments for proteins at ambient temperatures[29], the opposite trend is observed and atomic fluctuations increase as one goes from the core to the surface. Thus, solvent mobility determines the amplitudes of atomic fluctuations not only at the protein surface but also in the protein core. Interestingly, in the PC/SC and PH/SC simulations, the decrease of solvent mobility relative to the SH simulations leads to fluctuations of the core atoms that are essentially the same as in simulations with fixed solvent. This suggests, in agreement with results of Settles *et al.*[33], that at some point, as the solvent mobility decreases, the protein motions in the core become decoupled from the solvent.

The results of Nose-Hoover simulations indicate that it is mainly solvent mobility, regulated in our studies by the temperature (or by fixing the solvent molecules), that determines the magnitudes of protein fluctuations at and above 180 K. A series of Nose-Hoover simulations, where the solvent shell was coupled to a 300 K temperature bath and the protein temperature was decreased to below 180 K, showed that the effects due to the shape of the protein internal potential energy surface become significant at ~140 K; that is, the solvent shell with room temperature mobility is unable to induce large scale protein fluctuations when the protein is below that temperature. This agrees with the molecular dynamics simulations of Kuczera *et al.*[34], which showed that myoglobin in vacuum was confined to a single minimum at 80 K.

These simulations provide evidence concerning the atomic fluctuations that support the conclusion from experimental studies for the predominant role of solvent mobility in the protein 'glass' transition. This finding may have practical applications, such as trapping of productive enzyme intermediates[18] and turning protein function on or off at a given temperature for structural studies or for use in biotechnology[35].

Methods.

Nose-Hoover dynamic simulations. Carboxy myoglobin (MBCO) with a hydration shell of 492 waters was used for the Nose-Hoover simulation[28]. A slightly modified TIP3P model[36] was used to represent water molecules. No crystal waters from the myoglobin structure of Kuriyan *et al.*[37] were included. Water molecules were not constrained in the simulation[38] and were equilibrated as in Brooks *et al.*[13]. In Nose-Hoover simulations two separate temperature baths, each with coupling constant of 200 kcal mol^{-1} ps^2, were used to couple the protein and the surrounding water to different temperatures. It has been shown[28] that both the thermodynamics and dynamics obtained by use of the Nose-Hoover thermostat correspond to a canonical ensemble. In the present simulation the protein and solvent correspond to separate canonical ensembles at different temperatures in physical contact but with little heat conduction between them; the temperature at the boundaries is altered by no more than ±15 K relative to the value set by the Nose-Hoover thermostat (solvent and protein temperatures were monitored during the simulations). The crystal structure of MBCO by Kuriyan *et al.*[37] was used as the starting model for the simulations. Multiple bath Nose-Hoover dynamics, as implemented in CHARMM simulation program[39] was employed. The all-hydrogen topology with parameter set 22 was used. A switch function was used to truncate the van der Waals interactions over 10–12 Å and a shift function with a 12 Å cutoff was used to truncate the electrostatic interactions; a dielectric constant of 1 was used. An integration step of 0.001 ps was employed. Simulation at each set of Nose-Hoover coupling consisted of 50 ps equilibration and 100 ps production

Table 1 Average mean square fluctuations from the Nose-Hoover trajectories[1]

	PC/SC	PC/SH	PH/SC	PH/SH	PH/SH, fixed water
Mean square backbone fluctuations (Å^2)	0.09	0.18	0.09	0.23	0.051
Mean square non-hydrogen fluctuations (Å^2)	0.13	0.28	0.13	0.36	0.083
R.m.s. backbone bond length fluctuations (Å)	0.028	0.027	0.035	0.035	0.035
R.m.s. backbone bond angle fluctuations (°)	2.4	2.5	2.8	2.9	2.8
R.m.s. fluctuations of the distance between helices in van der Waals contact (Å)	0.18	0.24	0.20	0.25	0.10
R.m.s. fluctuations of the angles between helices in van der Waals contact (°)	1.3	1.7	1.3	2.0	0.91

[1]See Methods for description of procedures and the text for definition of PC, PH, SC, and SH.

dynamics. Coordinate frames were saved every 0.05 ps. Several simulations started with different coordinates showed that results are independent of the initial system configuration. Most of calculations were done on Hewlett-Packard 735/125 workstations.

Acknowledgments

We thank Y. Zhou and M.Watanabe for helpful discussions. This work is supported in parts by grants from the National Institute of Health to D.R. and M.K.

Correspondence should be addressed to M.K. *email: marci@tammy.harvard.edu*

Received 17 May, 1999; accepted 8 October, 1999.

1. Karplus, M. & Petsko, G.A. *Nature* **347**, 631–639 (1990).
2. Brooks III, C.L., Karplus, M. & Pettitt, B.M. *Proteins, A theoretical perspective of dynamics, structure, and thermodynamics.* (Wiley, New York; 1988).
3. Elber, R. & Karplus, M. *Science* **235**, 318–321 (1987).
4. Noguti, T. & Go, N. *Proteins* **5**, 104–112 (1989).
5. Frauenfelder, H., Sligar, G.S. & Wolynes, P.G. *Science* **254**, 1598–1603 (1991).
6. Angell, C.A. *Science* **267**, 1924–1935 (1995).
7. Sokolov, A.P. *Science* **273**, 1675–1676 (1996).
8. Iben, I.E.T. *et al*. *Phys. Rev. Lett.* **62**, 1916–1919 (1989).
9. Tilton, R.F., Dewan, J.C. & Petsko, G.A. *Biochemistry* **31**, 2469–2481 (1992).
10. Rasmussen, B.F., Stock, A.M., Ringe, D. & Petsko, G.A. *Nature* **357**, 423–424 (1992).
11. Doster, W., Cusack, S. & Petry, W. *Nature* **337**, 754–756 (1989).
12. Smith, J., Kuczera, K. & Karplus, M. *Proc. Natl. Acad. Sci. USA* **87**, 1601–1605 (1990).
13. Loncharich, R.J. & Brooks, B.R. *J. Mol. Biol.* **215**, 439–455 (1990).
14. Austin, R.H., Beeson, K.W., Eisenstein, L., Frauenfelder, H. & Gunsalus, I.C. *Biochemistry* **14**, 5355– 5373 (1975).
15. Parak, F., Frolov, E.N., Mössbauer, R.L. & Goldanskii, V.I. *J. Mol. Biol.* **145**, 825–833 (1981).
16. Lichtenegger, H. *et al. Biophys. J.* **76**, 414–422 (1999).
17. Laudat, J. & Laudat, F. *Europhys. Lett.* **20**, 663–667 (1992).
18. Ding, X., Rasmussen, B.F., Petsko, G.A. & Ringe, D. *Biochemistry* **33**, 9285–9293 (1994).
19. Ferrand, M., Dianoux, A.J., Petry, W. & Zaccai, G. *Proc. Natl. Acad. Sci. USA* **90**, 9668–72 (1993).
20. Norberg, J. & Nilsson, L. *Proc. Nat. Acad. Sci. USA* **93**, 10173–10176 (1996).
21. van Gunsteren, W.F. & Karplus, M. *Biochemistry* **21**, 2259–2274 (1982).
22. Brooks III, C.L. & Karplus, M. *J. Mol. Biol.* **208**, 159–181 (1989).
23. Beece, D. *et al. Biochemistry* **19**, 5147–5157 (1980).
24. Ansari, A., Jones, C.M., Henry, E.R., Hofrichter, J. & Eaton, W.A. *Science* **256**, 1796–1798 (1992).
25. Hagen, S.J., Hofrichter, J. & Eaton, W.A. *Science* **269**, 959–962 (1995).
26. Mayer, E. *Biophys. J.* **67**, 862–873 (1994).
27. Doster, W., Bachleitner, A., Dunau, R., Hiebl, M. & Luscher, E. *Biophys. J.* **50**, 213–219 (1986).
28. Hoover, W.G. *Phys. Rev. A* **31**, 1695–1697 (1985).
29. Petsko, G.A. & Ringe, D. *Ann. Rev. Biophys. Bioeng.* **13**, 331–371 (1984).
30. Swaminathan, S., Ichiya, T., van Gunsteren, W. & Karplus, M. *Biochemistry* **21**, 5230–5241 (1982).
31. Diehl, M., Doster, W., Petry, W. & Schober, H. *Biophy. J.* **73**, 2726–2732 (1997).
32. Ichiye, T. & Karplus, M. *Proteins* **11**, 205–217 (1991).
33. Settles, M., Post, F., Muller, D., Schulte, A. & Doster, W. *Biophys. Chem.* **43**, 107–116 (1992).
34. Kuczera, K., Kuriyan, J. & Karplus, M. *J. Mol. Biol.* **213**, 351–373 (1990).
35. Hagen, S.J., Hofricher, H.J., Bunn, H.F. & Eaton, W.A. *J. French Soc. Blood Trans.* **6**, 423–426 (1995).
36. Jorgensen, W.L., Chandrasekhar, J., Madura, J.D., Impey, R.W. & Klein, M.L. *J. Chem. Phys.* **79**, 926–935 (1983).
37. Kuriyan, J., Wilz, S., Karplus, M. & Petsko, G.A. *J. Mol. Biol.* **192**, 133–154 (1986).
38. Steinbach, P.J. & Brooks, B.R. *Proc. Natl. Acad. Sci.* **90**, 9135–9139 (1993).
39. Brooks, B.R. *et al. J. Comput. Chem.* **4**, 187–217 (1983).

The dodecameric ferritin from *Listeria innocua* contains a novel intersubunit iron-binding site

Andrea Ilari, Simonetta Stefanini, Emilia Chiancone and Demetrius Tsernoglou

CNR Center of Molecular Biology, Department of Biochemical Sciences "A. Rossi Fanelli", University La Sapienza, Piazzale Aldo Moro 5, 00185 Rome, Italy.

Ferritin is characterized by a highly conserved architecture that comprises 24 subunits assembled into a spherical cage with 432 symmetry. The only known exception is the dodecameric ferritin from *Listeria innocua*. The structure of *Listeria* ferritin has been determined to a resolution of 2.35 Å by molecular replacement, using as a search model the structure of Dps from *Escherichia coli*. The *Listeria* 12-mer is endowed with 23 symmetry and displays the functionally relevant structural features of the ferritin 24-mer, namely the negatively charged channels along the three-fold symmetry axes that serve for iron entry into the cavity and a negatively charged internal cavity for iron deposition. The electron density map shows 12 iron ions on the inner surface of the hollow core, at the interface between monomers related by two-fold axes. Analysis of the nature and stereochemistry of the iron-binding ligands reveals strong similarities with known ferroxidase sites. The *L. innocua* ferritin site, however, is the first described so far that has ligands belonging to two different subunits and is not contained within a four-helix bundle.

Nearly all forms of life require iron but must counter its unfavorable chemical properties that lead to formation of insoluble ferric-hydroxide polymers and toxic free radical species. Therefore iron is stored in ferritins that sequester the metal in a nontoxic and bioavailable form[1]. All ferritins share the same, highly conserved structure, with the exception of the protein extracted from *Listeria innocua*, the only known ferritin from a Gram-positive bacterium[2,3].

Typically, ferritins are oligomers of 24 identical or similar subunits (M_r 19–21 kDa) that assemble into a spherical shell (M_r 450–500 kDa, external diameter 120 Å) characterized by 432 symmetry[1]. The subunits share the same tertiary fold consisting of a four-helix bundle (helices A–D) with a fifth short helix (E helix) lying at an angle of about 60° to the bundle axis[4–6]. The apoferritin shell can store up to 4,500 iron atoms in the form of ferric hydroxy-phosphate micelles. However, incorporation of iron occurs when the metal is furnished to the protein as Fe^{2+} in the presence of molecular oxygen[1]. All natural ferritins therefore contain H-type subunits that carry within the four-helix bundle a highly conserved ferroxidase center that allows formation of a di-iron species, an intermediate in the iron oxidation and uptake process. Ferritins of higher vertebrates contain an additional type of subunit, called L, that forms hetero-oligomers with the H subunits. L-type chains do not possess a ferroxidase site, but contain a cluster of acidic residues that protrudes from the B helix into the apoferritin cavity and is thought to facilitate nucleation of the iron core[1].

Recently, Bozzi *et al.*[2] isolated from the Gram-positive bacterium *L. innocua* an oligomeric, spherical protein complex containing up to 50–100 iron atoms per oligomer and the functional properties of an authentic ferritin. Thus, at neutral pH values *Listeria* ferritin accelerates Fe^{2+} oxidation about four-fold with respect to auto oxidation[7]. This ferroxidase activity is about one third to one fourth that of mammalian recombinant H-chain ferritin[8,9] and *E. coli* bacterioferritin[10]. As in classical ferritins, the oxidized iron is sequestered inside the protein cav-